ELSEVIER

Journal of Power Sources 97–98 (2001) 13–21

JOURNAL OF POWER SOURCES

www.elsevier.com/locate/jpowsour

Aging mechanism in Li ion cells and calendar life predictions

M. Broussely[a,*], S. Herreyre[b], P. Biensan[b], P. Kasztejna[c], K. Nechev[c], R.J. Staniewicz[c]

[a]*SAFT BP 1039, 86060 Poitiers, France*
[b]*SAFT, 111 Blvd A. Daney, 33074 Bordeaux, France*
[c]*SAFT America, 107 Beaver court, Cockeysville, MD, USA*

Received 20 June 2000; received in revised form 23 January 2001; accepted 29 January 2001

Abstract

In this work, the long term calendar life of lithium ion cells for satellite and standby applications has been studied in experiments where the capacity evolution is tracked as a function of storage temperature. Cells containing either $LiCoO_2$ and $LiNi_xM_yO_2$ positives coupled with a graphite negative were float charged at 3.8 or 3.9 V. This study focused on losses at the negative electrode and the data were fit to a model which involved a rate-determining step governed by electronic conductivity of the solid electrolyte interphase (SEI) layer, following Arrhenius' law as a function of temperature. When nickel-based positives are used, a ''lithium reserve'' exists on the negative and this property enhances the calendar life for long life applications.

Keywords: Calendar life predictions; Aging reaction; Lithium ion batteries

1. Introduction

Lithium ion batteries in a short time span have captured the commercial markets for powering high-end electronics applications such as portable phones, camcorders, computers, etc. This was a natural outcome due to demonstrated excellent energy density and cycle life for these applications where the typical expected product life is probably 3–4 years. Other industrial applications, like standby power sources or satellites require very long life, typically more than 10 years, in difficult environmental conditions. Outstanding cycle life at small DOD has now been demonstrated [1,2]. However, the ability of Li ion cells to operate over very long time domains must still be demonstrated. Calendar life prediction for such cells must take into account possible aging reactions, with or without cycling, and almost no data to date has been reported. In order to evaluate the calendar life, different cell designs were tested in our laboratories over a period of time; the results are described and interpreted herein.

2. Experimental

High temperature was adopted as an expedient method to accelerate reaction rates within the cells so that cell-aging extrapolations could be made. Electrolyte reactions with electrode materials are the most probable parasitic reactions; therefore, a priori the most severe storage condition is the fully charged stated. This is particularly true for materials like lithiated metal oxides and lithiated amorphous or poorly crystallized carbons, which have an energy content that has strong voltage dependence. Another important point is that each electrode cannot be considered independently; indeed, reaction products formed on one electrode, and at least partly soluble in the electrolyte, could react on the other electrode, and influence the overall chemical stability of the system. Consequently, the best experimental conditions to perform calendar life should consist of having the cells stored at different temperatures and different voltages, corresponding to defined states of charge. The experiments described below were performed on cells containing either $LiCoO_2$ or $LiNiO_2$ electrode materials.

2.1. Common design

All cells were spirally wound and copper and aluminum foil were used for the negative and positive current collectors.

* Corresponding author. Tel.: +33-5-49-55-48-29; fax: +33-5-49-55-56-30.
E-mail address: michel.broussely@saft.alcatel.fr (M. Broussely).

0378-7753/01/$ – see front matter
PII: S0378-7753(01)00722-4

The microporous separator was PE/PP, while the electrodes had similar loadings and similar porosities. The positive electrode binder was PVDF, the negative binder was a non-fluorinated polymer and, the negatives were a mixture of two synthetic graphites.

2.2. Chemistries/design

2.2.1. MP Prototype

The "5 Ah" prismatic cell used a stainless steel can and was configured as can negative. The chemistry was $LiCoO_2$/EC-DEC-DMC 1 M $LiPF_6$ + VC additive/synthetic graphite.

2.2.2. High energy (HE) prototypes

The "40 Ah" cylindrical cell used a stainless can and was can negative. The chemistry was $LiNi_{0.81}Co_{0.09}O_2$/PC-EC-DMC 1 M $LiPF_6$ w/o additive/synthetic graphite.

2.2.3. HE industrial cell

The cell used an aluminum can, was produced on an industrial pilot line, and was configured as can positive. The chemistry was $LiNi_xM_yO_2$ ($x > 0.75$)/PC-EC-DMC 1 M $LiPF_6$ + VC additive/synthetic graphite.

2.3. Testing procedures

Cells were stored at different temperatures under constant applied voltage (called float potential). At defined periods of time, cell capacities were diagnosed either by discharging residual capacity at the storage temperature, or by charging the cell to the normal charge limit and discharging at ambient or high temperature.

3. Results

3.1. MP prismatic

Cells have been tested following a cross matrix involving four temperatures (15, 30, 40 and 60°C), and three voltages 3.8, 3.9 and 4.0 V. Three cells were tested for each condition. The cells are checked every month, after a 5 h charge at a constant current of 1.5 A (*C*/3), followed by a constant voltage step at 4.1 V to obtain the nominal capacity. Diagnostic discharge was made at 30°C using 0.94 A (*C*/5) to a 2.7 V cut-off. Fig. 1 shows, for example, the capacity evolution during float under 3.9 V at different temperatures. Each point represents the average of the three cells. Capacity decreases smoothly with a strong dependence on temperature and the loss rate tends to decrease with time. Fig. 2 shows the capacity loss evolution with time under different voltages at 30 and 60°C. It can be concluded that in these conditions, the capacity loss is mainly increased by temperature, although there is a lesser secondary influence of applied potential. At the same time, the cell impedance grows quite moderately, independent of the temperature, as shown in Fig. 3.

3.2. HE prototypes

Cells were stored at 3.8 V, at 30 and 60°C. They were checked every month, with the following sequence: (1) discharging the residual capacity at *C*/3; (2) charging at constant current C/3 + constant voltage at 4.0 V, ending at a total charge time of 5 h; (3) discharging the cell at 60°C at *C*/10; (4) charging the same way as previous sequence; (5) discharging the cells at 25°C at *C*/3 rate. The results are

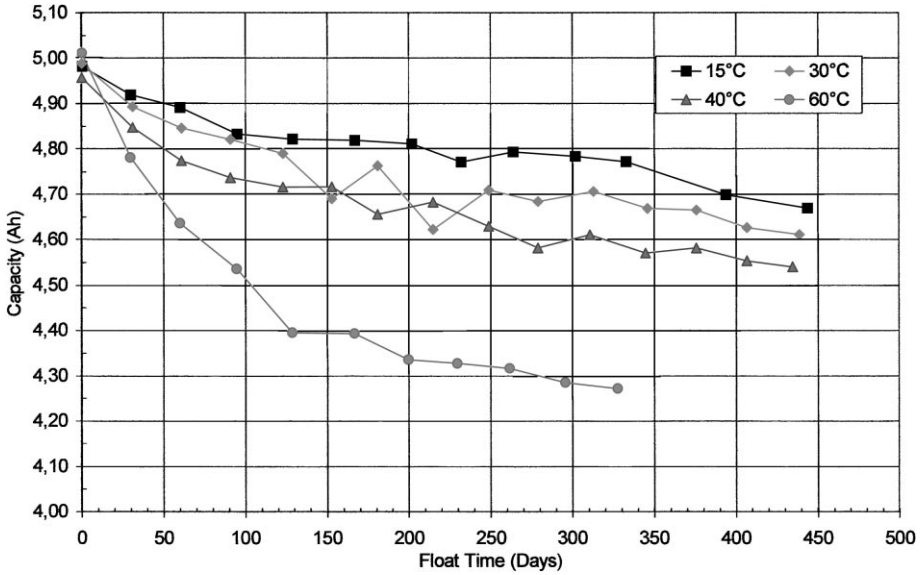

Fig. 1. Total capacity evolution of MP cells, measured monthly at 30°C-*C*/5, during storage under constant voltage of 3.9 V at different temperatures.

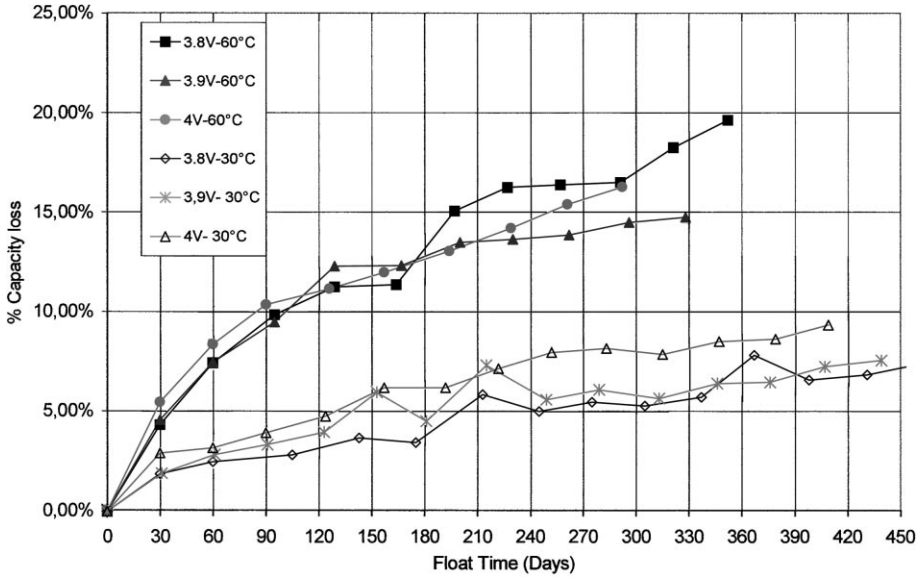

Fig. 2. Capacity loss on MP prototypes cells, measured at 30°C-*C*/3, during storage at 60 and 30°C under various voltages.

summarized in Fig. 4, which shows the capacity recovered every month after storage at 3.8 V float and 60°C (diagnostic discharges are performed at 60°C at *C*/10, and at 25°C at *C*/5).

The capacity evolution measured for the same cell is different when discharged at 25 or 60°C. While the 60°C capacity decreases continuously (similar to the $LiCoO_2$ MP cells at 30°C), the capacity obtained at 25°C is initially almost stable, and only starts to decrease at a 60°C after about four months. This specific behavior can be explained by considering the cell design and positive electrode discharge mechanism. It is well known that, unlike the lithium cobaltite, the nickel based lithiated oxides exhibit a first cycle efficiency smaller than 1, typically about 80%. A difference of 0.1–0.15 Li is not re-introduced during the first discharge, depending on the amount of Ni^{2+} in the crystalline phase [3]. Although some of the lithium is used to passivate the carbon, the remainder exists charged in the negative electrode, and the cell design must provide enough carbon to accommodate it. The result is that the cell is positive limited at the end of discharge, contrary to all other positive materials, whether manganese or cobalt oxide. However, when the discharge temperature increases and the rate decreases, all the lithium can be inserted again due to positive material properties, and the cell exhibits a higher and negative limited capacity. To summarize, the positive electrode at ambient temperature limits the cell, while the negative at high temperature limits it. This is very helpful to understand the mechanisms as described further in the discussion section. When cells are stored at 30°C, a

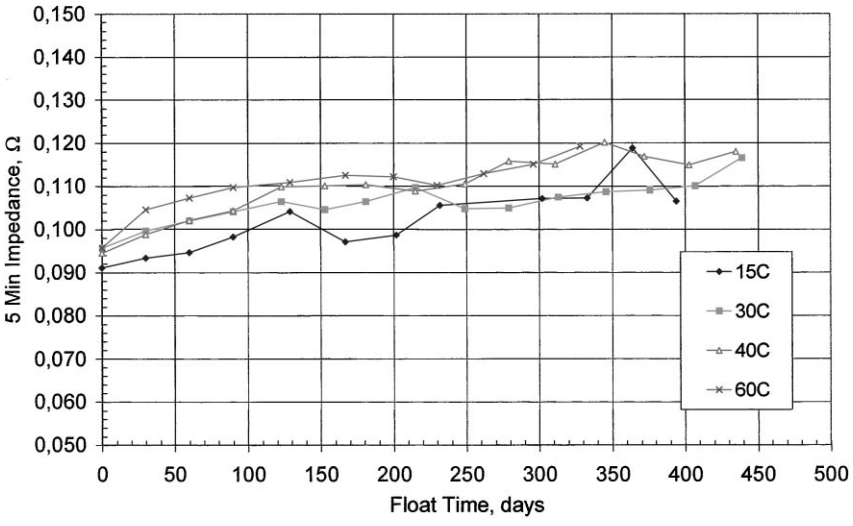

Fig. 3. Cell resistance (5 min voltage drop) evolution during floating at 3.9 V at different temperatures.

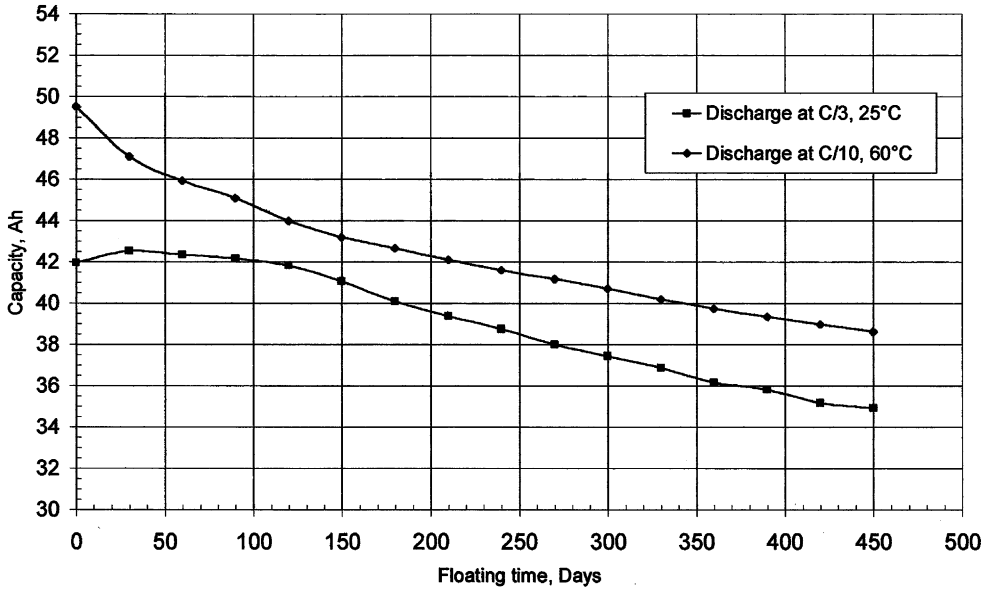

Fig. 4. HE cell prototype. Total capacity measured monthly using different discharge conditions after storage at 60°C and constant voltage of 3.8 V.

similar trend is observed, but the loss rate is much smaller, similar to that experienced with the MP cells. Fig. 5 shows the comparison of capacity variation measured at 60°C during storage at 3.8 V at 30°C. Two different cells are displayed, showing the reasonable reproducibility of the results.

3.3. HE industrial

As per the other test plans, cells were stored in "floating" conditions under constant voltage of 3.8 or 3.9 V, and at different temperatures following the description of Table 1. This particular test was launched to simulate standby applications, where voltages of 3.8 or 3.9 V are suitable for the overall battery voltage requirements. Three cells were grouped in parallel to get greater than 100 Ah capacity.

The cell capacity evolution is checked periodically by discharging at the floating temperature using 15 A to a 2.7 V cutoff to obtain the residual capacity of the cells. The results obtained so far are excellent, even at high temperature such as 60°C better than those obtained with the prototypes. At 40°C, no measurable loss is observed after about 1 year.

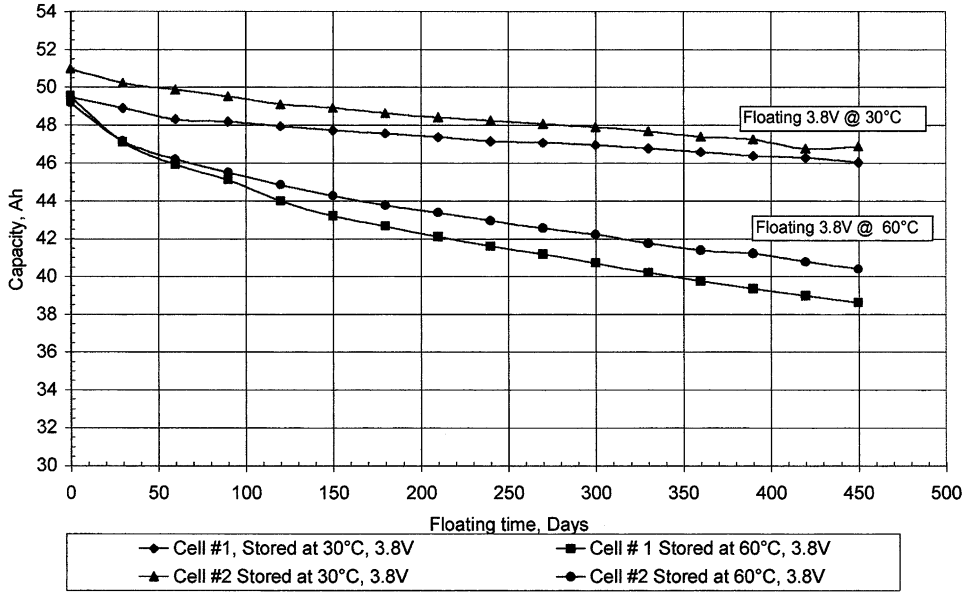

Fig. 5. HE prototype: total capacity evolution, measured monthly at 60°C-*C*/10 during storage at 30 or 60°C under constant voltage of 3.8 V.

Table 1
Capacity variation on float of HE industrial cells (three cells in parallel)[a]

Days	Module number				
	1 3.8 V (40°C)	2 3.8 V (60°C)	3 3.9 V (20°C)	4 3.9 V (40°C)	5 3.9 V (60°C)
0	105.7	107.7	116.5	121.6	125.9
90	105.5	105.9	116.2	121.9	122.6
120	106.2	104.5	115.7	120.4	121.8
180	106.4	103.4	115.9	122.6	121.1
240	106.0	102.8	117.4	120.5	120.1
300	104.2	102.0	120.0	121.5	119.1

[a] Floating conditions of voltage and temperature. Residual capacity at 15 A, measured at the floating temperature.

4. Discussion

The most common hypothesis for irreversible capacity loss during storage of a rechargeable cell involves side reactions between the electrolyte and the active materials. Oxidation on the positive, or reduction on the negative may occur, leading to capacity reduction. If these reactions occur simultaneously, the capacity loss may be reversible, as the equivalent part of the lithium lost on the negative electrode is re-inserted as Li^+ ions in the positive material. Indeed, reversible capacity losses are experienced with all the Li ion systems in the range of a few percent per month, depending on temperature, cell chemistries and design. The total amount of lithium involved is much greater than that originally contained in electrolyte, proving the interaction between the electrodes. This should be due to a ''shuttle'' mechanism, responsible for these reactions arising from the electrolyte itself, any impurities contained in the electrolyte, or other cell internal components within one of the active electrode. While the detailed mechanisms of such phenomenon is still under investigation, the purpose of the present work is to understand the mechanism of what could lead to irreversible losses; this situation is more of a concern for the users in long life applications. From Fig. 2 (describing the results obtained with the MP cells) it can be concluded that voltage has only a secondary influence on the capacity loss observed at high temperature. This indicates that the positive electrode is not the major actor, as its oxidation power depends directly on its charge voltage. In the same way, the results obtained with the nickel based cells (see Fig. 4) show clearly that, as long as the capacity is positive limited (when measured at ambient temperature), capacity stays almost stable, while when it is lithium limited (measured at 60°C), the capacity decreases in the same way as for cobalt based cells whose capacity is always limited by the negative electrode. Assumption of a capacity loss coming from an irreversible reaction occurring on the negative electrode and consuming lithium is then supported by the fact that, when all the lithium excess has been consumed, the measured capacity is then decreasing at similar rate, and the difference in absolute capacity values of the two measurements seems to remain constant. Temperature and rate account for this constant difference.

Negative electrodes, dismantled after more than 1 year floating at a charged state at 60°C, were rinsed with water, vacuum dried and, assembled in a coin cell versus Li. These recovered electrodes exhibited an ability to cycle lithium at the same initial specific capacity and polarization, thus, demonstrating the stability of the carbon structure. In the same way, the positive material on both cobalt and nickel based electrodes exhibited their starting crystalline structure (no modifications) and no additional phases were observed in the X-ray data. Some polarization increase observed on $LiNi_{0.81}Co_{.09}O_2$ electrodes may indicate that some reactions happened on this positive interface, but not affecting the total cell capacity measured at medium/low rate or high temperature conditions.

4.1. Lithium corrosion on negative electrode

Stability of all lithium batteries, including Li ion, results from the reduction of the electrolyte at the negative/electrolyte interface forming a passivation layer that remains conductive to Li^+ ions. The properties of this layer are crucial for the battery characteristics: if the reaction products are not passivating enough (i.e. insoluble, and adherent to the surface), the electrolyte molecules will continue to reach the reducing surface and lead to continued lithium corrosion. On the other hand, if the passivation layer is too thick or too poorly ionic (Li^+) conductive, cell internal resistance may increase to an unacceptable value. This is why only a few organic compounds can be used as solvent of electrolyte. This reasoning has been applied to all lithium batteries and has been extensively studied for many years. The most commonly adopted picture is that the interface layer is considered as a solid electrolyte interphase (SEI) being a good ionic but poor electronic conductor, as proposed by Peled [4].

As an example, the quest to make rechargeable metallic lithium cells has not been realized because of the continued reactivity of the lithium with the electrolyte (the

acknowledged failure mechanism), that is, during charge each new metal particle being plated reacts with the electrolyte to protect itself at ''its own expense'' (typically consuming about 1–2% each cycle). The lithium consumption problem is also a limiting factor for negative ''Li insertion'' electrodes in which volume variation during cycling is too high, destabilizing the SEI, which then has to be partly rebuilt each cycle.

The use of insertion carbon anode solves that problem, as the passivation layer is essentially complete after the first few charges and the small volume change between charged and discharged state does not significantly impair the mechanical stability of the SEI. Obviously, the long-term stability of this layer will have a primordial impact on the capacity retention, on aging, and on calendar life. A lot of work has been done to analyze the layer composition, for example, see [5,6]. As a simplified view, the layer is commonly accepted as being inhomogeneous with a ''multi-layer'' organization. While the external part is more or less porous and contains organic compounds like insoluble lithium alkyl carbonates, polyethylene, polypropylene, and lithium carbonate, the ''primary'' layer, very close to the carbon, would mainly be composed of inorganic species, lithium fluoride LiF (from reaction with $LiPF_6$) and Li_2CO_3. Total thickness is very small (in the range of tenth of a micron). Depending on the chain length, the alkyl carbonates may be more or less soluble, which can be the ''shuttle'' mentioned above, responsible for reversible self-discharge.

The condition of absolute stability, i.e. complete cessation of the electrolyte reduction implies that the electrons cannot move through the ''primary'' layer to reach the interface with the electrolyte. Li ions can obviously move through it easily, as this is the main cell reaction, which means that the layer should be electronically resistive.

The electronic resistance is not infinite and, we may expect that continuous slow electrolyte reduction will go on, thanks to this electron migration through the ''primary'' layer, which behaves as a semiconductor (''tunneling effect'') [7].

The following is a first attempt to model the lithium corrosion, i.e. capacity loss, which would be due to the parasitic reaction occurring between lithium in the carbon negative and the electrolyte. The kinetics of the reaction is assumed to be limited by the rate of electron transport, i.e. layer conductivity. We consider at initial time ''t_0'', the layer is essentially complete at the end of the formation step (1st charge). We need to stress the significant influence that the formation step has on the SEI properties and consequently on the future cell characteristics. Therefore, the formation procedure constitutes an important part of a manufacturers' know-how and the exact process may lead to a competitive advantage in terms of capacity stability.

As a first approach we may consider that the corrosion rate is limited by the electronic mobility of Li^+ in the layer, i.e. proportional to the SEI electronic conductance X:

$$\frac{dx}{dt} = kX = \frac{k\chi s}{e} \tag{1}$$

where x is the number of moles of Li being reacting, χ the specific conductivity, s the interface area and e is the layer thickness.

The corrosion reactions lead to different products, as discussed above. Some products are soluble (S) and create reversible self-discharge, which is compensated by an equivalent charging current (''floating current'') when a cell's state of charge is maintained by constant voltage. Whereas, insoluble products (I) trap the lithium, leading to irreversible capacity loss. In the following, x is the number of mole of Li irreversibly lost, following the rate of the Eq. (1).

The insoluble products are proportional to the number of Li moles (x) having reacted:

$$I = nx \tag{2}$$

The amount of insoluble products I leads to the layer building which means that the layer conductance will decrease with time and so should the corrosion rate.

The average layer thickness can be expressed as

$$e = e_0 + dI \tag{3}$$

where e_0 is the initial thickness after formation, and d is a constant coefficient linked to the average molar volume of the layer. And from Eqs. (2) and (3),

$$e = e_0 + dnx$$

simplified as

$$e = e_0 + Ax \tag{4}$$

Finally, Eq. (1) can be expressed as

$$\frac{dx}{dt} = kX = \frac{k\chi s}{e} = \frac{k\chi s}{e_0 + Ax}$$

and simplified as:

$$\frac{dx}{dt} = \frac{B}{e_0 + Ax}$$

or

$$(e_0 + Ax)\,dx = B\,dt$$

Integration, with $x = 0$, at $t = 0$ leads to the equation:

$$\tfrac{1}{2}Ax^2 + e_0x - Bt = 0$$

i.e. the relation between time t and corrosion x:

$$t = \frac{A}{2B}x^2 + \frac{e_0}{B}x \tag{5}$$

with

$$A = dn$$

$$B = k\chi s$$

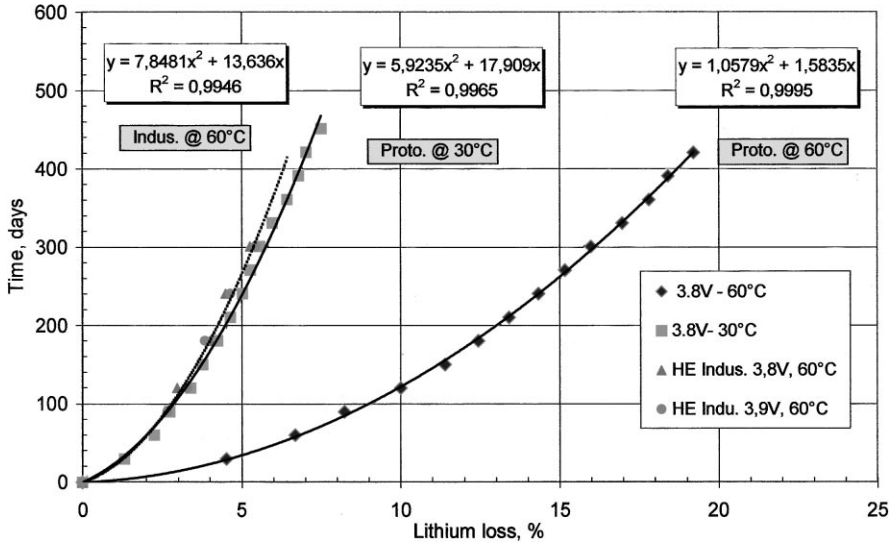

Fig. 6. Time of storage as a function of lithium loss, for HE cells on storage under 3.8 or 3.9 V constant voltage at 60 or 30°C. Agreement with a parabolic model is judged by the R^2 fit.

and t is the time elapsed from initial, after formation, x is the amount of Li corroded. The constant parameters are: χ is the Specific conductivity, s the interface area considered, e_0 the layer thickness, and k, n and d are coefficients of proportionality.

From these constants, χ only increases with temperature.

4.2. Comparison with actual data

The model was first compared to the HE prototypes data shown in Fig. 6, using the average of the individual values of the two cells for the 30°C and 60°C storage conditions. The curve-fitting coefficient is excellent, which gives credit to the model. Data from Industrial HE cells of Table 1 at 3.8 and 3.9 V are also reported in Fig. 6. These results also fit very well with the model, with a much smaller corrosion rate: the Li loss at 60°C is similar to that obtained at 30°C on prototypes. In addition to changes in cell chemistry (the positive material and use of VC additive in the electrolyte), this improvement could also be due to a better control of manufacturing process, and smaller level of impurities, which may have a drastic influence on layer conductance properties. The same exercise can be made with MP cells results, as described in Fig. 7. Due to the smaller capacity of the cell and accuracy of the discharge equipment, there is a larger scattering of the results. However, a parabolic shape is

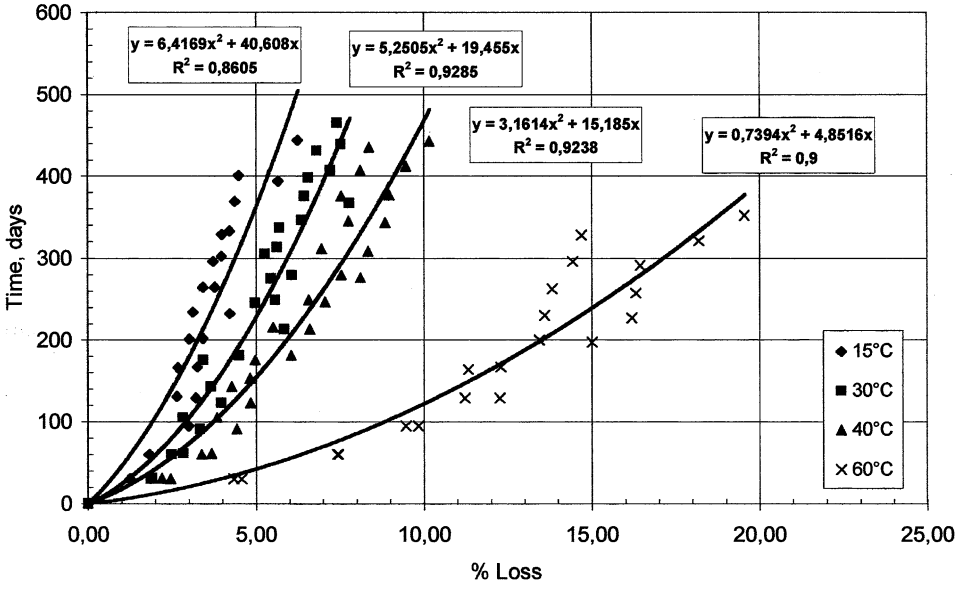

Fig. 7. Time of storage as a function of lithium loss, for MP prototypes cells on storage under 3.8 or 3.9 V constant voltage at four temperatures. Agreement with a parabolic model is judged by the R^2 fit.

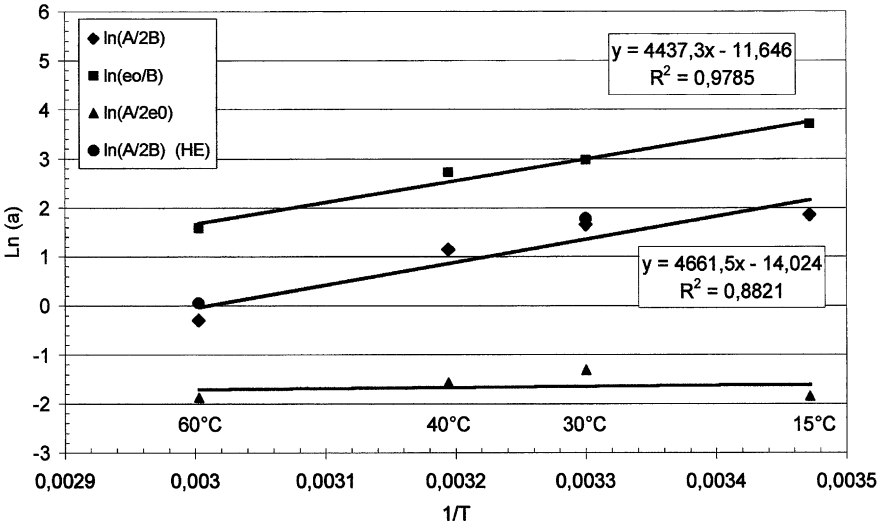

Fig. 8. Variation of the logarithm of the coefficients with temperature for MP cells.

also followed quite reasonably, and interestingly with coefficients similar to the HE prototypes in spite of different chemistry.

Looking at the moderate increase in the MP cell resistance in Fig. 3, means there is only a small increase in the ionic resistance of the SEI. Continued growth of the SEI induces a large increase in electronic resistance of the primary layer that, in turn, slows down the direct reaction of solvent at electrode interface.

4.3. Effect of temperature and calendar life predictions

It is usual to consider the temperature coefficient on the capacity loss rate as exponential, following an Arrhenius law:

$$K = K_0 e^{-ER/T}, \quad \text{or} \quad \log K = \ln K_0 - \frac{E}{RT}$$

where E is similar to activation energy. In the present case, we can apply the Arrhenius law to the coefficients B and A of the equation of corrosion rate (see above):

$$\frac{dx}{dt} = \frac{B}{[e_0 + Ax]}$$

where $B = k\chi s$, is proportional to the layer electronic conductivity χ. This conductivity variation with temperature is consistent with a semiconductor-type, which should obviously be the case of the layer conductivity. $A = dn$ should not vary with temperature, as well as initial thickness e_0 (formed at the same temperature).

We can then consider the variation of coefficients of Eq. (5) with temperature, $\ln(A/(2B))$ and $\ln(e_0/B)$, from the fitted equations in Fig. 7 of MP prototypes. Linear equations as a function of $1/T$ are obtained as shown on Fig. 8, and the absence of significant variation of the logarithm of the coefficient ratio, $\ln(A/2B) - \ln(e_0/B) = \ln(A/2e_0)$, confirms the hypothesis that electronic conductance of the layer is the rate determining factor.

The values of $(A/2B)$ coefficient (which is the most influent) from the HE cells have been added in Fig. 8, at 30 and 60°C, showing similar behavior.

From the slopes of the lines, we can therefore, determine equation of the conductivity as a function of temperature:

$$\ln\left[\frac{A}{(2B)}\right] = \frac{4661}{T} - 14;$$

$$\ln(B) = \ln(k\chi s) = -\frac{4461}{T} + 14 + \ln(A) - \ln(2)$$

and

$$\ln\chi = -\frac{4461}{T} + [13.3 + \ln(A) - \ln(k) - \ln(s)]$$

This assumes all terms between the brackets are independent of temperature.

In the same way, we can obtain from the coefficient (e_0/B):

$$\ln\chi = -(4437/T) + [11.6 - \ln(k) - \ln(s) + \ln(e_0)]$$

The value of E, similar to an activation energy, should be identical from both equations. The less than 5% difference can be considered as quite acceptable, taking in account to the relative precision of the results.

A general equation can be deduced, to calculate lithium corrosion curves as a function of time, at different temperatures, and make extrapolations for longer period of time.

$$t = e^{[(4661/T)-14]}x^2 + e^{[(4437/T)-11.6]}x$$

Fig. 9 gives the representation of the simulation between 10 and 60°C, extrapolating the curves until large amounts of lithium have corroded. The data obtained with HE prototypes cells, described in Fig. 6, have been plotted in the graph for comparison, which shows that the two cell designs

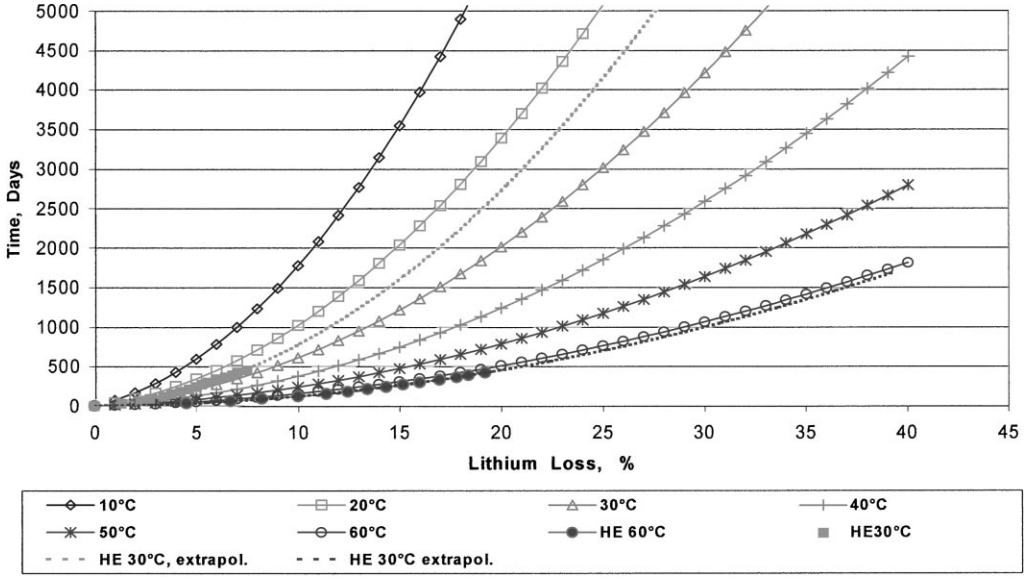

Fig. 9. Simulation of Li corrosion (time vs. % Li corroded) as a function of time and temperature obtained from data on MP prototypes cells. Curves obtained from HE prototypes cells (Fig. 5), and their extrapolations are added for comparison.

and chemistries behave similarly, as pointed out before. A high temperature 60°C curve fits quite well.

These extrapolations are valid for any given design and chemistry provided the data is collected from storage experiments. If a new chemistry is adopted, then storage experiments have to be performed again to deduce the new rate coefficients. This model is very useful for assessing calendar life predictions solely due to losses at the negative electrode and from the fitted curves; extrapolations can be made for end-of-life estimates.

At this point, it is interesting to note the unique property of the nickel based systems: due to the mechanism explained in previous section, an excess of about 12% of nominal capacity remains as charged Li in the negative at the end of normal discharge conditions. This ''free'' lithium can be corroded with time, before having any impact on practical cell capacity. As a result, the time to reach a given end of life would be extended by this reserve. For example, from Fig. 9, time to reach 80% of nominal capacity after continuous storage at 40°C would increase from 1200 days (20%loss in $LiCoO_2$ cells) to 2700 days (32% with Ni based system).

5. Conclusions

From this study, it can be concluded that the lithium oxidation on the negative electrode is a major side reaction affecting the cell capacity on storage at high temperature. When graphite is used for the negative electrode, this phenomenon is not greatly influenced by cell voltage, since the negative electrode voltage varies little as a function of state of charge. As a cell ages, the production of insoluble species on the graphite modifies the SEI properties, leading to a reduction of the corrosion rate with time. A model involving a rate-determining step governed by electronic conductivity of the layer fits quite well with the experimental data and calendar life predictions may be deduced, especially for high temperature. This first study has focused on the negative electrode while the role of the positive electrode needs further study and verification. Certainly, mechanisms such as the oxidative reactions of the positive may produce other side reactions that result in additional losses on storage at high voltage. The case of reversible self-discharge must also involve the positive electrode reduction.

Results obtained today with the SAFT high energy Li ion design produced on an industrial pilot line, predict an outstanding calendar life capability, enhanced by the unique property of the nickel-based oxides to provide a ''lithium reserve''.

References

[1] R.J.Staniewicz, L. d'Ussel, P. Kasztenjna, W. Gollatz, in: Proceedings of the SAE Aerospace Power Systems (P-341), April 1999, Mesa, AZ, p. 149.
[2] R.J. Staniewicz, in: Proceedings of the Space Power Workshop, April 2000, Torrance, CA.
[3] C. Delmas, J.P. Peres, A. Rougier, A. Demourgues, F. Weill, A. Chadwick, M. Broussely, F. Perton, P. Biensan, P. Willmann, J. Power Sources 54 (1995) 329.
[4] E. Peled, J. Electrochem. Soc. 126 (1979) 2047.
[5] D. Aurbach, B. Markowsky, I. Weissman, E. Levi, Y. Ein-Eli, Electrochim. Acta 45 (1999) 67–86.
[6] R. Yazami, Electrochim. Acta 45 (1999) 87–97.
[7] E. Peled, in: J.P. Gabano (Ed.), Lithium Batteries, Academic Press, NY, 1983, pp. 43–72.